Atomic transfer through interfacial free volumes in $Sn_{65.4}Bi_{34.6}$ eutectic systems

2008 J. Phys.: Condens. Matter 20 395234

(http://iopscience.iop.org/0953-8984/20/39/395234)

J. Phys.: Condens. Matter **20** (2008) 395234 (5pp) doi:10.1088/0953-8984/20/39/395234

Atomic transfer through interfacial free volumes in $Sn_{65.4}Bi_{34.6}$ eutectic systems

K Sato[1], H Murakami[1], K Fujimoto[1], M Nakata[2], T Oka[3] and Y Kobayashi[3]

[1] Department of Environmental Sciences, Tokyo Gakugei University, 4-1-1 Koganei, Tokyo 184-8501, Japan
[2] Department of Astronomy and Earth Sciences, Tokyo Gakugei University, 4-1-1 Koganei, Tokyo 184-8501, Japan
[3] National Institute of Advanced Industrial Science and Technology (AIST), 1-1-1 Higashi, Tsukuba, Ibaraki 305-8565, Japan

E-mail: sato-k@u-gakugei.ac.jp

Received 29 May 2008, in final form 22 August 2008
Published 4 September 2008
Online at stacks.iop.org/JPhysCM/20/395234

Abstract

Atomic transfer through the interfaces upon Bi precipitation is specifically investigated with respect to vacancy-sized free volumes for a $Sn_{65.4}Bi_{34.6}$ eutectic alloy of a highly heterogeneous system by making full use of backscattering electron imaging, small-angle x-ray scattering, x-ray diffraction, and positron annihilation spectroscopy. Bi-rich particles of ∼100 nm with segregated nanocrystallites of ∼30 nm are observed for the alloy cooled at a cooling rate of 10^{-1} K s^{-1}. Bi particles and nanocrystallites intergrow with each other up to ∼1 μm and ∼55 nm, respectively, by an extremely slow cooling of 10^{-5} K s^{-1}. Regardless of the cooling rate, high concentrations of vacancy-sized free volumes are found to be located at interfaces among short-range ordered phases. For the alloy cooled at 10^{-1} K s^{-1}, the free volumes are dominantly surrounded by Bi atoms. Decreasing the cooling rate down to 10^{-5} K s^{-1} changes the free volumes with Bi-rich chemical surroundings to an Sn-rich environment, which directly indicates atomic transfer through the interfaces upon Bi precipitation. The present results demonstrate that the kinetics of vacancy-sized free volumes in the interfaces plays an important role in understanding the precipitation mechanism in nanostructured heterogeneous materials.

1. Introduction

Nanostructured heterogeneous materials, as represented by nanocomposites, have attracted attention due to their unique functionality and mechanical and magneto-optical properties [1]. In these materials there exist structurally and compositionally different phases with wide size variations, separated by interfaces that are variant in composition and structure. Such phenomena as, for example, segregation, intergrowth, nanoprecipitation, and nanophase separation originating from nanoscale heterogeneity involve atomic transfer through the interfaces. Advanced techniques such as the three-dimensional atom probe [2], small-angle x-ray scattering (SAXS) [3], high resolution transmission electron microscopy (TEM) [4], positron annihilation spectroscopy [5], and tracer diffusion experiments [6] have been applied for probing local atomic structures in nanostructured heterogeneous materials.

The Sn–Bi eutectic alloy system is one of several typical heterogeneous materials. Owing to its low melting temperature, the Sn–Bi eutectic alloy without any toxic elements has been accepted as a potential candidate for environmentally friendly solders [7, 8]. In Bi-containing eutectic alloys there often appears Bi precipitation during cooling, which is macroscopically visible [9]. Bi particles grow with decreasing the cooling rate [10, 11]. The Bi precipitation considerably deteriorates the mechanical property of the alloy [7, 12]. In our previous work using positron annihilation spectroscopy, vacancy-sized free volumes in interfaces among certain short-range ordered regions were observed [13]. In the present study, the local atomic structures for the $Sn_{65.4}Bi_{34.6}$ eutectic alloy system are further investigated by making full use of backscattering electron (BE) imaging, SAXS, x-ray diffraction (XRD), and positron annihilation spectroscopy.

2. Experiment

Pure elements of Sn and Bi with nominal composition of $Sn_{65}Bi_{35}$ at.% were melted and several specimens were cut from the same ingot. Electron probe microanalysis (EPMA) revealed a chemical composition of $Sn_{65.4}Bi_{34.6}$. A melting temperature of 412 K was determined by differential scanning calorimetry (DSC). The specimens were heated up to 398 K and then cooled at different cooling rates of 10^{-1}, 10^{-3}, and 10^{-5} K s^{-1}.

BE imaging [14] was performed at room temperature for ingot specimens cooled at the three cooling rates. Average sizes of Bi-rich particles were estimated directly from BE images. SAXS measurements [15] with Mo Kα radiation were performed at room temperature for powder specimens. XRD measurements with Cu Kα radiation were performed at room temperature for powder specimens. The average sizes of Bi crystallites were evaluated from the Bi(012) peak broadening by employing Scherrer's formula [16].

Positron lifetime and coincident Doppler broadening spectroscopy were performed for specimens cooled at the three cooling rates. The positron source (^{22}Na), sealed in a thin foil of Kapton, was mounted in a sample–source–sample sandwich for the lifetime and coincident Doppler broadening measurements. Positron annihilation lifetime spectra ($\sim 1 \times 10^6$ coincidence counts) were recorded with a time resolution of 230 ps full-width at half-maximum (FWHM) at room temperature. The data were numerically analyzed using the POSITRONFIT code [17]. Coincident Doppler broadening spectroscopy was performed by measuring the energies of the two annihilation quanta E_1 and E_2 with a collinear set-up [18] of two high-purity Ge detectors with 1.0 keV (FWHM) energy resolution. The spectra were obtained by cutting the E_1, E_2 spectra along the energy conservation line $E_1 + E_2 = (1022 \pm 1)$ keV, taking into account the annihilation events within a strip of $\pm$ 1.6 keV [19].

3. Results and discussion

Figure 1 shows BE images of $Sn_{65.4}Bi_{34.6}$ cooled at different cooling rates (1) 10^{-1} K s^{-1}, (2) 10^{-3} K s^{-1}, and (3) 10^{-5} K s^{-1}. There appear bright parts arising from the electron backscattering effect from particles of higher atomic numbers (see arrows in figure 1). Since the atomic number of Bi (83) is much higher than Sn (50), we reasonably ascribe bright parts to Bi-rich particles. They substantially grow with decreasing the cooling rate. Extremely slow cooling with 10^{-5} K s^{-1} yields surprisingly huge Bi-rich particles exceeding 1 μm in size. The sizes of Bi-rich particles estimated from BE images are listed in table 1.

Figure 2 shows SAXS profiles obtained for $Sn_{65.4}Bi_{34.6}$ cooled at (1) 10^{-1} K s^{-1}, (2) 10^{-3} K s^{-1}, and (3) 10^{-5} K s^{-1}. Scattered x-ray intensities $I(Q)$ are presented as a function of scattering vector $Q = 4\pi \sin(\theta/2)/\lambda$ defined by scattering angle θ and x-ray wavelength λ. With decreasing the cooling rate, SAXS intensity in the low Q region attributable to the scattering from Bi-rich particles is strongly enhanced, in agreement with the results of BE imaging (see table 1).

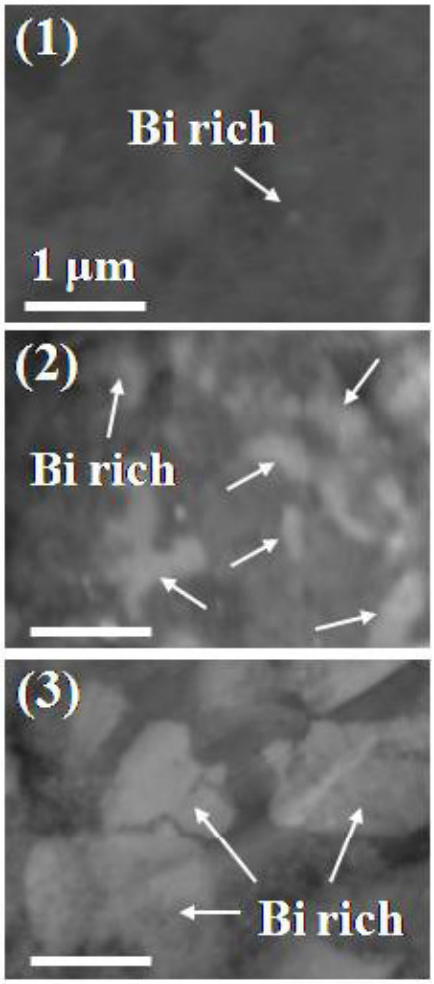

Figure 1. Backscattering electron images of $Sn_{65.4}Bi_{34.6}$ cooled at cooling rates of (1) 10^{-1} K s^{-1}, (2) 10^{-3} K s^{-1}, and (3) 10^{-5} K s^{-1}. The magnification factor is 40 000$\times$ for all images. Bright parts indicated by arrows are the resultants from Bi precipitation.

Table 1. Average size of Bi-rich particles in $Sn_{65.4}Bi_{34.6}$ cooled at cooling rates of (1) 10^{-1} K s^{-1}, (2) 10^{-3} K s^{-1}, and (3) 10^{-5} K s^{-1} evaluated from the data of backscattering electron (BE) images. The table includes Bi crystallite sizes evaluated from x-ray diffraction (XRD).

Cooling rate (K s^{-1})	BE imaging (nm)	XRD (nm)
(1) 10^{-1}	100 ± 30	34 ± 3
(2) 10^{-3}	600 ± 50	48 ± 4
(3) 10^{-5}	1000 ± 80	55 ± 6

Figure 3 shows XRD patterns measured for $Sn_{65.4}Bi_{34.6}$ cooled at cooling rates of (1) 10^{-1} K s^{-1}, (2) 10^{-3} K s^{-1}, and (3) 10^{-5} K s^{-1} together with the calculated intensities. Diffraction peaks are well indexed with those of body-centered tetragonal β-Sn and rhombohedral Bi phases, signifying an eutectic structure of β-Sn and Bi. We note here that Bi(012) peaks are narrower in the order of (3) 10^{-5} K s^{-1}, (2) 10^{-3} K s^{-1}, and (1) 10^{-1} K s^{-1}. This demonstrates that the Bi crystallite grows with decreasing cooling rate (see figure 3 (c)). Average sizes of Bi crystallites evaluated from the Bi(012)

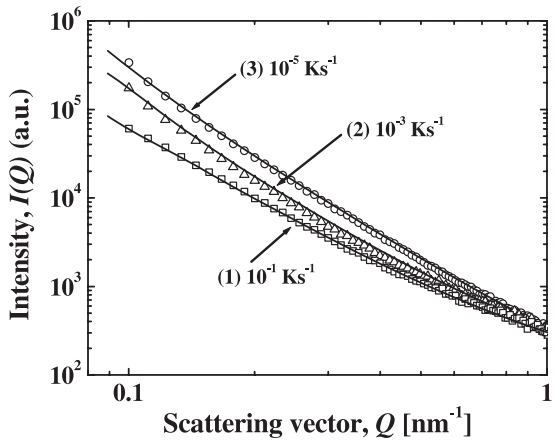

Figure 2. Small-angle x-ray scattering profiles of $Sn_{65.4}Bi_{34.6}$ cooled at cooling rates of (1) 10^{-1} K s^{-1}, (2) 10^{-3} K s^{-1}, and (3) 10^{-5} K s^{-1}. Solid lines are drawn to guide the eye.

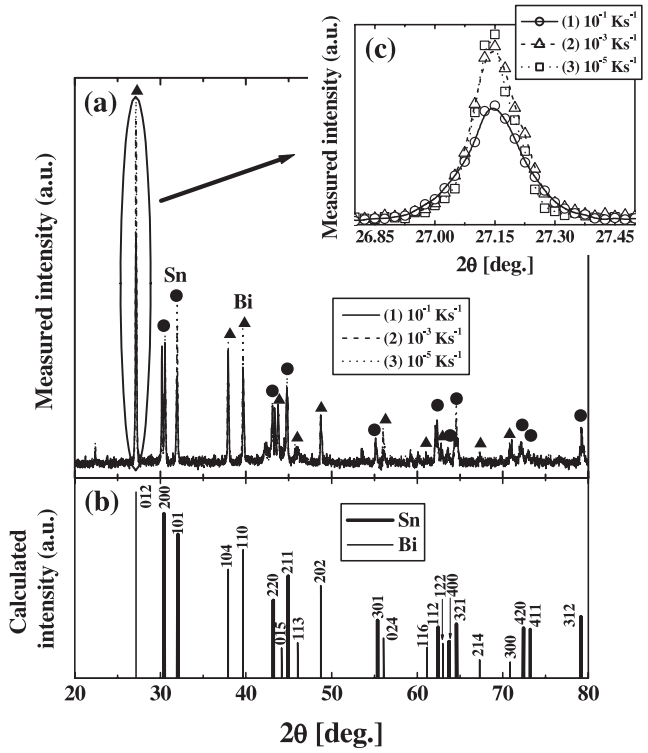

Figure 3. (a) Measured XRD patterns of $Sn_{65.4}Bi_{34.6}$ cooled at cooling rates of (1) 10^{-1} K s^{-1} (solid line), (2) 10^{-3} K s^{-1} (dashed line), and (3) 10^{-5} K s^{-1} (dotted line). XRD peaks indexed to the body-centered tetragonal Sn and rhombohedral Bi phases are marked with solid circles and triangles, respectively. (b) Calculated XRD patterns. Thick and thin lines correspond to the diffraction from Sn and Bi, respectively. (c) Enlarged section of Bi(012) peaks.

peak broadening by employing Scherrer's formula are listed in table 1.

It is reported that cooling rate sensitively influences the microstructure and mechanical property of Bi-containing eutectic alloys [10, 11]. Lowering the cooling rate increases the size of Bi-rich particles and the mechanical property is deteriorated. In the present study we observed the increase of

Table 2. Positron lifetimes of $Sn_{65.4}Bi_{34.6}$ cooled at cooling rates of (1) 10^{-1} K s^{-1}, (2) 10^{-3} K s^{-1}, and (3) 10^{-5} K s^{-1}. Experimental uncertainty is $\Delta\tau = \pm 3$ ps. Positron lifetimes in the free state (τ_f) and positron lifetimes in monovacancies (τ_v) of the β-Sn and Bi are given for comparison. Note that the positron lifetime of $Sn_{65.4}Bi_{34.6}$ decreases with decreasing cooling rate.

Specimen	Cooling rate (K s^{-1})	τ_1 (ps)	τ_2 (ps)
(1) $Sn_{65.4}Bi_{34.6}$	10^{-1}	—	274
(2) $Sn_{65.4}Bi_{34.6}$	10^{-3}	—	267
(3) $Sn_{65.4}Bi_{34.6}$	10^{-5}	—	254
		τ_f (ps)	τ_v (ps)
β-Sn	—	205 [17]	242 [17]
Bi	—	225 [18]	258 [19]

the particle size upon lowering the cooling rate for $Sn_{65.4}Bi_{34.6}$ by BE imaging and SAXS. On the other hand, the average size of Bi crystallites evaluated from XRD data is one order of magnitude smaller than the particle size obtained by BE imaging. This provides us evidence that the segregation of Bi nanocrystallites occurs inside the Bi-rich particles. The increase of the crystallite size with decreasing cooling rate shows that Bi nanocrystallites and Bi-rich particles intergrow with each other.

In order to gain insight into the atomistic transport processes underlying the intergrowth segregation, positron annihilation spectroscopy was conducted. Positron lifetime spectroscopy yields a single component as listed in table 2 [13]. Observed positron lifetimes are much longer than the defect-free matrix of β-Sn (205 ps) [20] and Bi (225 ps) [21], and rather close to the values of a β-Sn monovacancy (242 ps) [20] and Bi monovacancy (258 ps) [22]. We therefore conclude the presence of concentrated vacancy-sized free volumes over 10^{-4} in concentration, giving rise to positron saturation trapping [23]. Judging from the highly heterogeneous structures of the present $Sn_{65.4}Bi_{34.6}$ eutectic system as confirmed by XRD experiments, positron trapping into the interfaces among short-range ordered phases is most probable.

It should be noted here that the positron lifetime significantly decreases with decreasing the cooling rate. As can be seen in table 2, the positron lifetimes in both the free state and monovacancy for pure Bi are much longer than those of β-Sn. The decrease of positron lifetime is most probably due to the change of chemical environment around the free volumes [13], as described below.

BE images and SAXS data show that Bi-rich particles grow upon lowering the cooling rate. The evolution of the interface underlying the precipitation of Bi-rich particles can be specifically detected by coincident Doppler broadening spectroscopy. In figure 4, the ratio spectra normalized to the Al spectrum are presented to highlight the differences among the different cooling rates. At (1) 10^{-1} K s^{-1}, the Doppler broadening ratio spectrum indicates a significant peak around $38 \times 10^{-3} m_0 c$ characteristic of annihilation with Bi atoms. This demonstrates that the positron trapping vacancy-sized free volumes are dominantly surrounded by Bi atoms. The decrease of the cooling rate down to (2) 10^{-3} K s^{-1} weakens the peak,

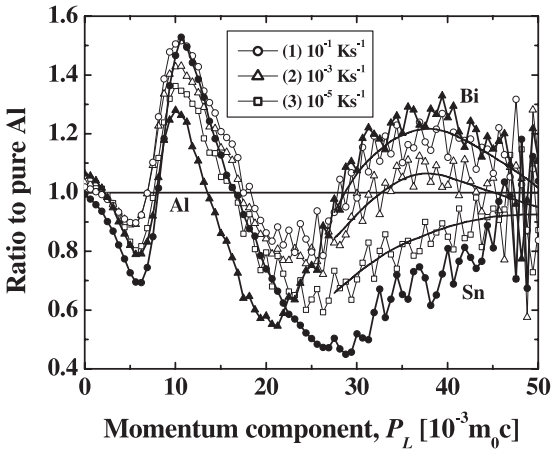

Figure 4. Coincident Doppler broadening spectra of $Sn_{65.4}Bi_{34.6}$ cooled at cooling rates of (1) 10^{-1} K s^{-1} (open circles), (2) 10^{-3} K s^{-1} (open triangles), and (3) 10^{-5} K s^{-1} (open squares) together with those of pure Sn (solid circles) and pure Bi (solid triangles). Each spectrum is normalized to the Doppler broadening spectrum of pure Al ($Y = 1$). The solid lines in the core electron region are drawn for guiding the eye.

signaling the change of chemical surrounding around the free volumes from Bi to Sn atoms. At (3) 10^{-5} K s^{-1}, any feature of the peak is no longer observed and the spectral shape is rather close to the Sn spectrum, indicating that more Sn atoms are present around the free volumes. The above results reveal that atomic transfer through the free volumes is responsible for the precipitation of the Bi-rich particles. At the lowest cooling rate of 10^{-5} K s^{-1}, a large number of Bi atoms transferred from the interface lead to the formation of the large particles.

We now relate the macroscopic scattering data by BE imaging and SAXS to the data of nanoscopic structure by XRD and positron annihilation spectroscopy. With the intergrowth of Bi particles and Bi nanocrystallites upon decreasing the cooling rate, chemical surroundings around free volumes at the interfaces are changed from a Bi- to Sn-rich environment. Cooling rate dependence of the macroscopic Bi precipitation could be associated with the kinetics of free volumes at interfaces. Cooling with 10^{-1} K s^{-1} is fast enough to quench the microstructure and Bi atoms are thus not provided to Bi particles. Hence the Bi-rich particles are rather small in size. By lowering the cooling rate down to 10^{-3} and 10^{-5} K s^{-1}, their chemical surroundings are changed from a Bi to Sn-rich environment due to considerable transfer of Bi atoms, which makes the Bi-rich particles grow to an extremely large size.

4. Conclusion

The influence of the cooling rate on local atomic structure was investigated for the $Sn_{65.4}Bi_{34.6}$ eutectic alloy of a highly heterogeneous system both on the macroscopic and nanoscopic scale by making full use of backscattering electron (BE) imaging, small-angle x-ray scattering (SAXS), x-ray diffraction (XRD), and positron annihilation spectroscopy. BE imaging revealed Bi precipitation with a particle size of ∼100 nm for the alloy cooled at 10^{-1} K s^{-1}. The Bi particles were segregated into Bi nanocrystallites with a size of ∼34 nm as confirmed by XRD. With decreasing cooling rate, Bi particles and Bi nanocrystallites intergrow with each other. An extremely slow cooling with 10^{-5} K s^{-1} generates Bi particles of huge sizes of approximately ∼1 μm, which contain Bi nanocrystallites of ∼55 nm. It is found that there exist high concentrations of vacancy-sized free volumes at the interfaces among short-range ordered phases. For the alloy cooled at 10^{-1} K s^{-1}, the free volumes are dominantly surrounded by Bi atoms. With decreasing the cooling rate down to 10^{-5} K s^{-1}, the free volumes with Bi-rich chemical surroundings are changed to an Sn-rich environment. The present results furnish direct evidence that atomic transfer through the interfaces occurs via vacancy-sized free volumes upon macroscopic Bi precipitation.

Acknowledgments

Fruitful discussions with Professor H-E Schaefer (Universität Stuttgart) are acknowledged. This work was supported by the New Energy and Industrial Technology Development Organization (NEDO) and a Grant-in-Aid of the Japanese Ministry of Education, Science, Sports, and Culture (Grant Nos 18840016, 18560651, and 20740173).

References

[1] For example, Murakami Y, Yoo J H, Shindo D, Atou T and Kikuchi M 2003 *Nature* **423** 965
[2] Ohkubo T, Miyoshi T, Hirosawa S and Hono K 2007 *Mater. Sci. Eng.* **449–451** 435
[3] Narayanan S, Lee D R, Hagman A, Li X and Wang J 2007 *Phys. Rev. Lett.* **98** 185506
[4] Babonneau D, Pailloux F, Eymery J-P, Denanot M-F, Guerin Ph, Fonda E and Lyon O 2005 *Phys. Rev.* B **71** 035430
[5] Sato K, Murakami H, Kobayashi Y, Sprengel W and Schaefer H-E 2007 *J. Non-Cryst. Solids* **353** 1882
[6] Herth S, Eggersmann M, Eversheim P-D and Würschum R 2004 *J. Appl. Phys.* **95** 5075
[7] Mitlin D, Raeder C H and Messler R W 1999 *Metall. Mater. Trans.* A **30** 115
[8] Reinikainen T and Kivilahti J 1999 *Metall. Mater. Trans.* A **30** 123
[9] Kim Y-S, Kim K-S, Hwang C-W and Suganuma K 2003 *J. Alloys Compounds* **352** 237
[10] da Silveria A F, de Castro W B, Luciano B A and Kiminami C S 2004 *Mater. Sci. Eng.* A **375–377** 473
[11] Khalifa B A, Nagy M R and Afify R 2005 *Phys. Status Solidi* a **202** 55
[12] Chuang C M, Lui T S and Chen L H 2002 *J. Mater. Sci.* **37** 191
[13] Sato K, Murakami H and Kobayashi Y 2008 *New J. Phys.* submitted
[14] For example, Zheng L and Tao T 2006 *Rare Met.* **25** 231
[15] For example, Myers R T, Cohen R E and Bellare A 1999 *Macromolecules* **32** 2706
[16] For example, Correia J B, Marques M T, Carvalho P A and Vilar R 2007 *J. Alloys Compounds* **434/435** 301
[17] Kirkegaard P and Eldrup M 1974 *Comput. Phys. Commun.* **7** 401
[18] Asoka-Kumar P, Alatalo M, Ghosh V J, Kruseman A C, Nielsen B and Lynn K G 1996 *Phys. Rev. Lett.* **77** 2097

[19] Sato K, Shanai D, Hotani Y, Ougizawa T, Ito K, Hirata K and Kobayashi Y 2006 *Phys. Rev. Lett.* **96** 228302
[20] Herlach D, Stoll H, Trost W, Metz H, Jackman T E, Maier K, Schaefer H-E and Seeger A 1977 *Appl. Phys.* **12** 59
[21] Clayton J M, Usmar S G, Fretwell H M, MacKenzie I K and Alam M A 1995 *J. Phys.: Condens. Matter* **7** 3181
[22] Lemahieu I, Dorikens-Vanpraet L, Segers D, Dorikens M, Moser P, Corbel C and Bois P 1987 *Phys. Status Solidi* a **102** 659
[23] Puska M J and Nieminen R M 1983 *J. Phys. F: Met. Phys.* **13** 333